Physica Scripta. Vol. T16, 119–126, 1987.

Prospects for Alpha Particle Studies on TFTR

S. J. Zweben

Princeton Plasma Physics Laboratory, Princeton, New Jersey, U.S.A.

Received June 24, 1986; accepted June 30, 1986

Abstract

TFTR is expected to produce approximately 5 MW of alpha heating during the D/T $Q \approx 1$ phase of operation in 1989–1990. At that point the collective confinement properties and the heating effects of alpha particles become accessible to study for the first time. This paper outlines the potential performance of TFTR with respect to alpha particle production, the diagnostics which will be available for alpha particle measurements, and the physics issues which can be studied both before and during D/T operation.

1. Introduction

This paper aims to give a general overview of the physics and diagnostics of alpha particles in TFTR. The study of alpha particles will naturally be divided into two phases: the pre-tritium phase during which "single-particle" effects can be observed with the 3.7 MeV alphas created in the D/^{3}He reaction (or with other charged fusion products), and the D/T phase during which the population of alphas will be ≈ 1000 times higher and "collective" effects may begin to appear. At the TFTR goal of $Q \approx 1$ alpha heating will contribute $\approx 20\%$ to the global plasma power balance, at which point some hints about ignited plasma behavior might be obtained.

In Section 2 the performance of TFTR with respect to alpha particle creation and confinement will be described, both at the machine's present "single-particle" level and at its projected $Q \approx 1$ level to be obtained with the addition of tritium in 1989–1990. In Section 3 the potential diagnostics for TFTR alpha particle studies are outlined, and in Section 4 the alpha physics issues accessible for study in TFTR are briefly reviewed.

2. Alpha particle creation and confinement properties of TFTR

The basic creation and classical confinement properties of alpha particles in tokamaks are simple and well known. This section reviews these properties in the context of TFTR.

2.1. *"Single-particle" creation at $Q \ll 1$*

Alpha particles and other alpha-like fusion products can be created at relatively low levels without the explicit addition of tritium to the discharge. In particular, the 3.7 MeV alpha created in D/^{3}He reactions is nearly identical to the 3.5 MeV alpha particle created in D/T reactions, although its maximum creation rate is only about 10^{-3} that of D/T alphas (assuming predominantly beam-target reactions at 100 keV deuterium beam energy). The 3.7 MeV alpha can also be created during ^{3}He minority heating [1].

As shown in Table I, there are several other charged fusion products which can also be used to simulate single-particle alpha effects. The 1.0 MeV triton and 3.0 MeV proton created

Table I. *Fusion products in TFTR*

Fusion reactions:

D + T = n(14 MeV) + α(3.5 MeV)
D + D = n(2.5 MeV) + ^{3}He (0.8 MeV)
= T(1 MeV) + p(3 MeV)
D + ^{3}He = p(15 MeV) + α(3.7 MeV)

Fusion product	Maximum production rate (s^{-1})[a]	Typical toroidal gyroradius (cm)[b]	Typical 1/e slowing down time (s)[c]
3.5 MeV α	$\gtrsim 10^{19}$	5.4	0.35
3.7 MeV α	$\sim 10^{15}$–10^{16}	5.7	0.35
1.0 MeV T	$\gtrsim 10^{16}$	5.0	1.1
3.0 MeV p	$\gtrsim 10^{16}$	5.0	0.35
0.8 MeV ^{3}He	$\gtrsim 10^{16}$	2.3	0.26
15 MeV p	$\sim 10^{15}$–10^{16}	11.2	0.35

[a] Beam-target reaction rate at $E_b \cong 100$ keV and $P_b \cong 25$ MW.
[b] Evaluated assuming 90° pitch angle at 50 kG.
[c] For slowing down to 1/e of initial energy, assuming $T_e = 10$ KeV and $n = 10^{14}$ cm^{-3}.

radius as the 3.5 MeV D/T alpha, and have a diagnostic advantage over the 3.7 MeV D/^{3}He alpha in that their creation rate can be monitored by the associated 2.5 MeV neutron (whereas the 15 MeV proton and 17 MeV gamma associated with the D/^{3}He reaction are more difficult to detect). Note that actual D/T alphas are also created in TFTR without the explicit addition of tritium through the "burnup" of 1 MeV tritons as they slow down in a background of deuterium; however, the number of these alphas is only about 1% of the number of tritons created, so that they are relatively difficult to detect.

Thus there are several fusion products accessible for study in TFTR which can simulate D/T alpha particles even at $Q \ll 1$. In the next section the expected single-particle confinement properties of these particles are described.

2.2. *Single-particle alpha confinement at $Q \ll 1$*

At the production levels described above for pre-tritium TFTR operation, the alphas and other charged fusion products will almost certainly not affect the plasma, so that they may be considered to be test particle "probes" of the discharge's alpha confinement properties. The expected single-particle confinement of alphas in TFTR has been calculated theoretically [2–5], and these theoretical models have already been incorporated into computer codes which can calculate alpha confinement for specific TFTR configurations.

The basic criterion for single-particle confinement is that the excursion of the alpha particle drift orbit from the magnetic flux surface "δ" should be less than the distance between

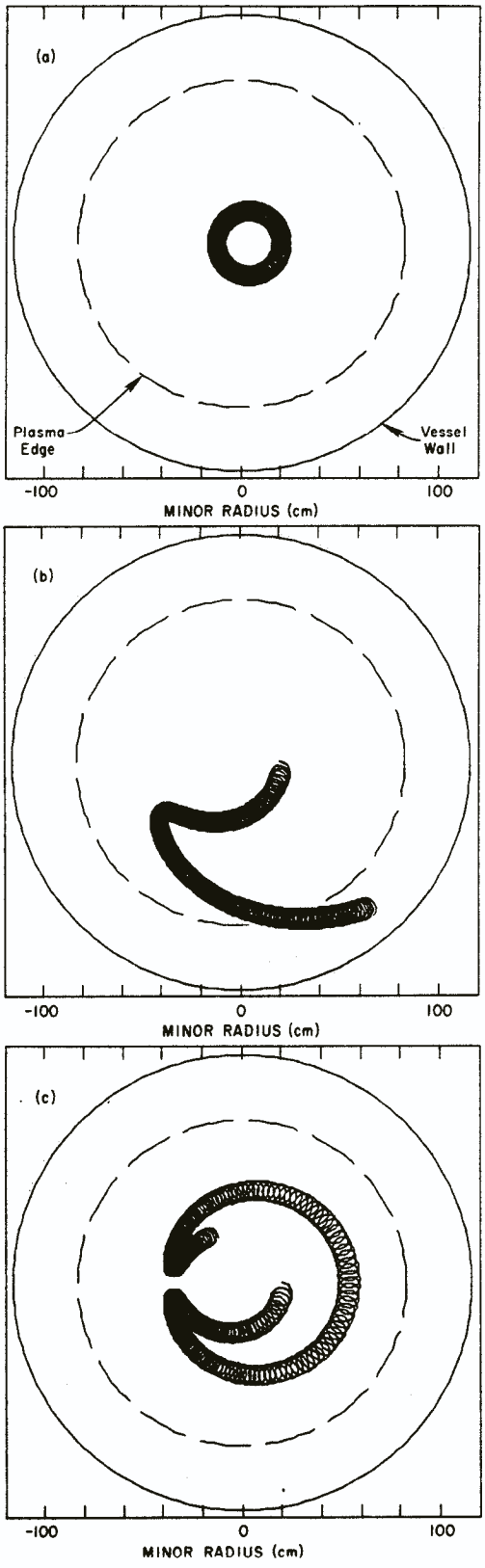

Fig. 1. Typical alpha particle orbits in TFTR. Each particle is started out at the outer equatorial plane at a radius of $r/a = 0.25$ in a plasma with a parabolic-cubed current profile. In (a) the plasma current is 1.5 MA and the initial pitch angle is 60° (co-going), in (b) the plasma current is also 1.5 MA but the initial pitch angle is −60°, and in (c) the plasma current is 3.0 MA and the initial pitch angle is the same as for (b), showing the improved con-

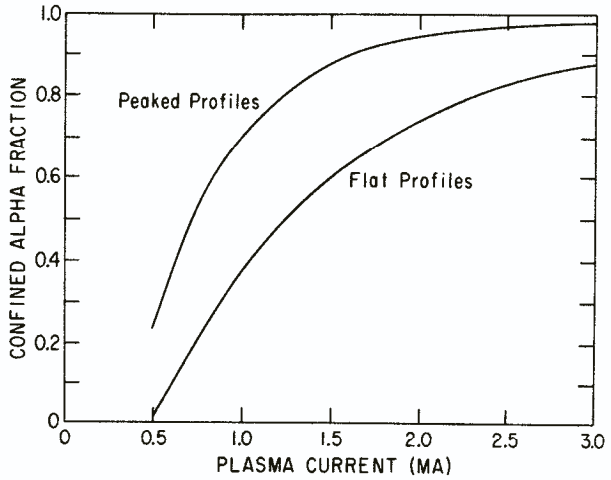

Fig. 2. Confined alpha fraction vs plasma current in TRTR. The upper curve is obtained assuming plasma current profile of parabolic-to-the-forth and an alpha source profile of parabolic-to-the-sixth (peaked profiles), while the lower curve is obtained assuming first and second order parabolic profiles, respectively (flat profiles). Over the operational range of 0.5–3 MA in TFTR the confined alpha fraction should vary considerably.

varies inversely with the plasma current, and also depends on the particle's pitch angle (with respect to the toroidal field) and to a lesser extent on the plasma current profile. For a typical alpha particle, roughly:

$$\delta/a \approx \rho_{\text{pol}}/R \tag{1}$$

where a and R are the plasma minor and major radii and ρ_{pol} is the alpha's gyroradius evaluated in the poloidal field.

In Fig. 1 are some examples of calculated 3.5 MeV alpha particle orbits in TFTR. In Figs. 1(a) and 1(b) are trajectories for particles born at $r/a = 0.25$ in a plasma of moderate current $I = 1.5$ MA at a toroidal field of 50 KG. Case (a) shows that an alpha born at this point with a pitch angle of 60° (co-going) is well confined on its first orbit, while case (b) shows that an alpha born at the same place but with a pitch angle of −60° escapes to the wall on its first orbit. Figure 1(c) shows that by increasing the plasma current in the latter case to 3 MA the previously escaping orbit becomes well confined, due to its decreased excursion from the flux surface on which it was born.

In Fig. 2 are code calculations by Heidbrink of the expected fraction of confined alphas in TFTR vs. plasma current, based on the model of Ref. [2]. At the lowest available currents in TFTR less than half of the alphas are confined on their first orbit, while at the highest available currents of 3 MA up to 95% of the alphas are confined on their first orbit. Note that this calculated fraction depends upon the assumed radial profile of alpha creation and on the assumed plasma current profile. With a more peaked source profile the fraction of confined alphas is larger since the alphas born near the plasma center are generally better confined, while for a more peaked plasma current profile the fraction of confined alphas is larger since the most alphas are born near the center, and the local orbit excursion decreases with increased local poloidal field.

After its first orbit the alpha slows down primarily on electrons while losing energy without appreciable pitch angle scattering over a slowing-down timescale of τ , where roughly

[5]:

$$\tau_{s,e}(s) \approx 1.2 \times 10^{12} T_e^{3/2}(\text{keV})/n(\text{cm}^{-3}). \quad (2)$$

During this time the alpha's excursion from the flux surface gradually decreases due to its decreasing momentum, such that alphas that were well confined on their first orbit should generally stay confined until they have thermalized.

There are also some "non-prompt" alpha losses after the first orbit, particularly for those particles born near the pitch angle for maximum loss [2]. As calculated by Hively for TFTR, these losses should be approximately 1% of the confined alpha population for typical TFTR parameters, i.e., typically 10% of the escaping particle losses at $I \approx 2.5$ MA. Non-prompt losses can be distinguished from prompt first-orbit losses by the energy of the escaping alpha, since the energy loss during the first orbit is negligible.

Note that these expectations for alpha particle confinement in TFTR come from the simplest "classical" single-particle confinement and thermalization models. More subtle physical effects associated with non-axisymmetric magnetic fields and plasma instabilities are discussed in Section 4. However, this classical model comprises the basic alpha physics usually incorporated into tokamak modelling codes.

2.3. *Alpha particles at $Q \approx 1$ in TFTR*

There are various computer simulations of the D/T $Q \approx 1$ phase of TFTR, all of which are necessarily speculative since the confinement properties of full beam power TFTR discharges are not yet known. However, in order to anticipate the relevant physics and to prepare the appropriate diagnostics, it is useful to know the range of alpha particle effects expected for typical $Q \approx 1$ scenarios.

In Table II are three typical TFTR $Q \approx 1$ simulations as calculated with the BALDUR code by Mikkelsen [6]. These cases differ mainly by their assumed plasma density, which is an experimental parameter that can be controlled relatively easily. The first case at the lowest density corresponds to the "energetic-ion" or "high-T_i" mode routinely obtained in TFTR at low density and high beam power. The second case simulates a moderately high density, normally gas-puff fueled, beam-heated discharge. The third case at the highest density adds pellet fueling and 7 MW of ICRF heating to simulate recent upgrades to the anticipated TFTR performance. Note that these three cases do not use the same confinement model, and so cannot be directly compared to one another however, they do all have $Q \approx 1$ and alpha heating power in the 4–5 MW range.

Table II. *TFTR $Q \approx 1$ scenarios*

	Low n	Medium n	High n
Run No.	TQR111	TJQ009	TJQ052
I_p (MA)	2.5	2.5	3.0
B_T (T)	5.2	5.2	5.2
$\bar{n}$ (10^{14})	0.51	0.74	1.1
P_{beam} (MW)	27	28	28
P_{RF} (MW)	–	–	7
Heating (s)	2	2	2
Z_{eff}	~1.5	~1.5	~1.2
$n(0)$ 10^{14} cm^{-3}	0.65	1.1	2.1
$T_i(0)$ (keV)	41	20	12.8
$T_e(0)$	13	9.2	7.4
$\langle\beta\rangle$ (%)	2.2	1.6	1.4
$\tau_E(a)$ (s)	0.36	0.27	0.18
$\beta(0)_{tor}$ (%)	4.5	4.4	6.0
$\langle\beta_z\rangle$ (%)	0.26	0.11	0.04
P_α (MW)	4.4	4.8	3.8
$P_{\alpha,lost}$ (MW)	0.5	0.4	0.1
$\tau_E(a/2)$ (s)	0.38	0.34	0.23
$n(0)\,T_i(0)\,\tau_e(a/2)$ (10^{18} cm^{-3} eV s)	0.99	0.7	0.6
Q_{inst}	1.0	1.0	0.55
(%) beam-target	40	35	18

Radial profiles of various alpha-related quantities for these three simulations are shown in Fig. 3. In Fig. 3(a) are the calculated fast alpha density profiles (for $E_\alpha > 3/2T_i$), along with the fraction of alphas which are lost on their first orbit, (assuming wall radius = plasma radius), showing that almost all alphas are confined, at least according to the classical alpha confinement model used in this code. This figure and also Fig. 3(b) show that the fast alpha density is highest in the lowest density case; this is simply due to the longer slowing down time at the lower densities (and higher electron temperatures), as shown in Fig. 3(c). The fast alpha beta is also largest in the lowest density case for the same reason, since the average fast alpha energy is approximately constant (≈ 1 MeV) in the classical slowing down model. The thermalized alpha density is highest at the highest density, however, since the alphas accumulate over more slowing down times in this case (and are modeled to remain on the flux surfaces of their birth in this code).

Thus for typical $Q \approx 1$ scenarios in TFTR the expected central fast alpha densities and betas are in the range 2–7 $\times 10^{11}$ alphas/cm^3 and 0.3–0.8%, respectively. Note that these are upper limits in the sense that non-classical losses might also occur, as discussed in Section 4.

In Fig. 3(f) is shown the ratio of alpha heating to total plasma loss (excluding the losses due to sawteeth) vs. radius. In none of these simulations is this ratio significantly above the global value of $P_\alpha/P_{loss} \approx 0.2$ expected for $Q \approx 1$ (note that the highest density case has an assumed central ICRF heating power deposition which reduces the relative importance of alpha heating in this region). Thus alpha heating would be expected to play a relatively minor (but potentially measurable) role in the power balance of these discharges.

2.4. *Alpha particle simulation with neutral beams or ^{3}He tails*

Some aspects of alpha particle physics might be simulated in TFTR using the large fast ion populations obtained with injected 100 keV deuterium beams or with resonantly heated ^{3}He minority tails [7]. In both cases the single particle confinement properties of these ions are probably similar to those of alphas of the same momentum.

Although the distribution functions of these ions are not identical to the expected isotropic alpha slowing down distribution function, an understanding of the collective instability properties of these fast ion populations might eventually be useful in developing theory appropriate to alphas in ignited plasmas. Note that in both cases the fast ion populations obtained by direct heating are comparable to or larger than the fast alpha populations obtainable at $Q \approx 1$.

2.5. *Central ignition scenarios*

Since alpha particles should be well contained and quickly thermalized in TFTR, it should be possible (at least in prin-

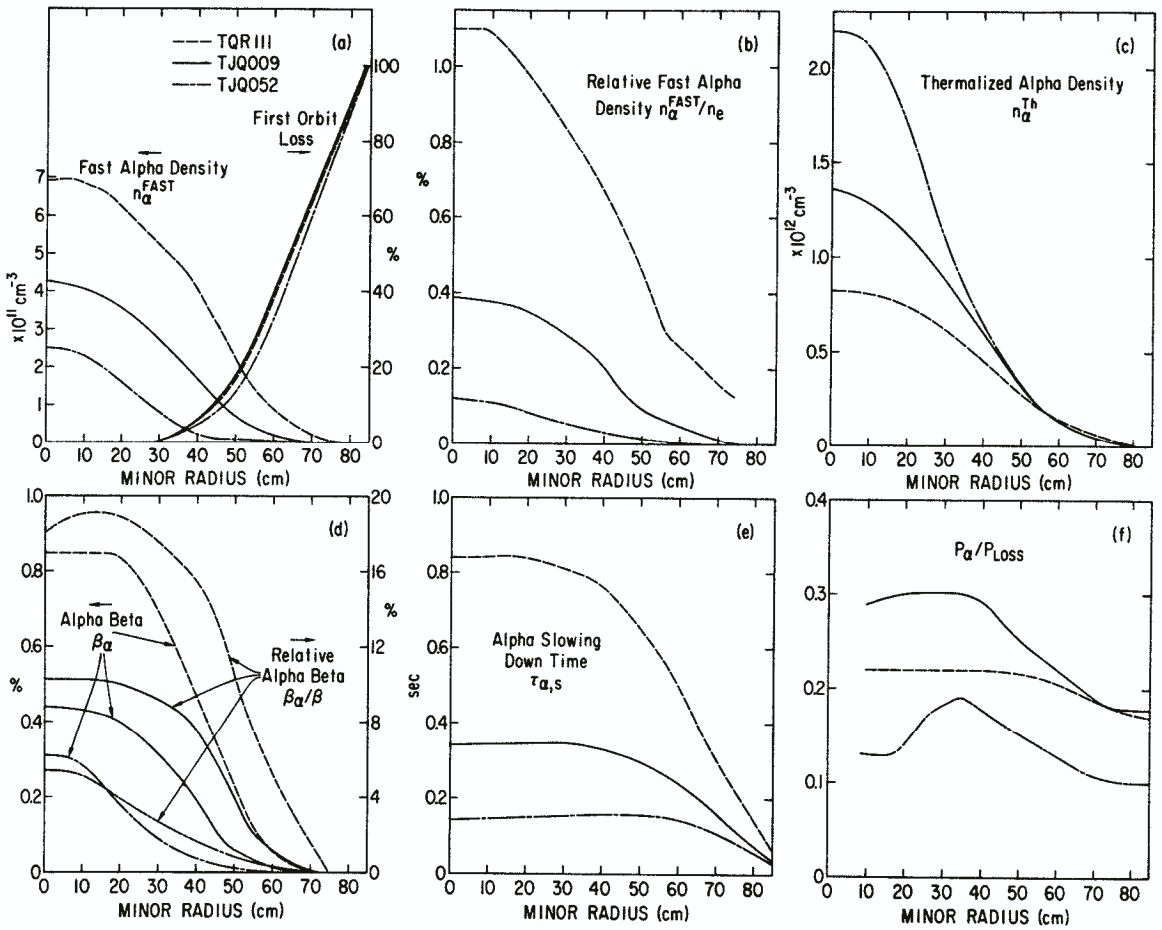

Fig. 3. Computer code simulations of alpha particle related quantities for typical $Q \approx 1$ scenarios in TFTR. These three scenarios differ mainly in the plasma density, but all have 4–5 MW of alpha heating near $Q \approx 1$ (see also Table II). The lowest density case TQR111 has the highest alpha density and alpha beta since the alpha slowing down time is longest.

sustained ignition. The conventional limits to TFTR performance as expressed in Table II are set by the empirical anomalous confinement properties and the empirical density and beta limits observed in tokamaks over the past few years; in particular, the confinement anomaly of typically 10–100 with respect to the ion neoclassical limit allows the possibility for substantial improvement in TFTR performance.

The requirements for obtaining central ignition in TFTR have been discussed recently using simplified estimates and BALDUR simulations [8], where by central ignition is meant $P_\alpha/P_{loss} = 1$ within some region near the center of the discharge. The requirement for central ignition is given roughly by $n(0)\,T_i(0)\,\tau_E(0) \approx 3 \times 10^{18}\,\mathrm{cm}^{-3}\,\mathrm{eV\,s}$ at $T_i(0) \approx 10\,\mathrm{keV}$. If these central conditions can be obtained with peaked density profiles (typically $n(0)/\bar{n} \cong 2.7$), then the resulting average densities and betas are less than a factor of two above their empirical limits. Thus a possible approach to central ignition in TFTR is similar to that described by the third case in Table II, but with a central confinement time of ≈ 1 s instead of the assumed 0.23 s in that simulation. It remains to be seen whether the long central confinement times obtained recently in TFTR with pellet injection can be sustained at high central temperature.

3. Alpha particle diagnostics

Prospects for alpha particle diagnostics have improved gradually over the past few years [9]. This section will review the diagnostics available for TFTR without touching on the longer-range diagnostic possibilities applicable to the next-generation ignited tokamaks.

3.1. *Escaping alphas*

Escaping alphas can be detected relatively easily using techniques analogous to those developed for escaping 3 and 15 MeV protons on PLT and PDX [10, 11]. The principal difficulty derives from the need to replace the standard silicon surface barrier diode with a detector suitable for use in the harsh neutron environment at $Q \approx 1$ in TFTR.

A prototype inorganic scintillator detector compatible with this required level of radiation resistance has been installed recently on TFTR [12]. It consists of *an* $\approx 10\,\mu$ microcrystalline layer of ZnS(Ag) onto which escaping alphas, tritons, and protons impact after having passed through a 3 μm aluminum foil shield. These impacts produce visible scintillations which are fiberoptically coupled to photomultiplier tubes for either pulse or flux counting. For

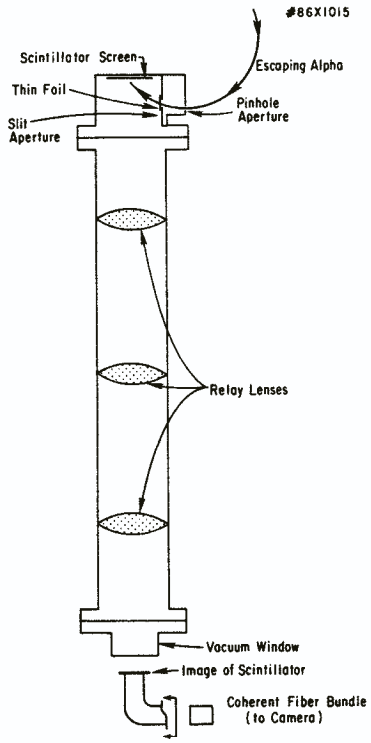

Fig. 4. Design of an escaping alpha detector for TFTR. The alphas (or other fusion products) are separated by the entrance apertures according to their pitch angle in one dimension and their energy (gyroradius) in the other dimension. The image of their impact on the scintillator screen in transferred to an intensified video camera for analysis.

3.5 MeV alphas and 1.0 MeV tritons the counting efficiency of this detector is nearly 100%, while for neutrons and gammas the efficiency should be $\approx 10^{-4}$ and 10^{-6}, respectively.

A more advanced version of this detector is shown schematically in Fig. 4. Alphas and other fusion products pass successively through a pinhole and slit aperture [1] which disperses the particles onto the 2-D scintillator screen according to their pitch angle and gyroradius (energy). The scintillator screen is then imaged onto a coherent fiber bundle and the image is recorded with an intensified video camera. An array of detectors similar to this is planned for installation on TFTR in 1987. Simpler modular detectors will also be installed at various points on the vessel wall to monitor possible anomalous or ripple-induced losses.

Other possible escaping alpha detectors are described in Ref. [9].

3.2. *Charge exchange recombination spectroscopy*

Slow confined alphas with energies up to ≈ 500 keV can be diagnosed spectroscopically through a single-charge exchange process between the alpha and the 80 keV diagnostic neutral beam [13]. The technique has already been used to measure thermal helium atoms at a density of $\approx 10^{12}\,\mathrm{cm}^{-3}$ in PDX, which is about the density expected for thermalized alphas at $Q \approx 1$ in TFTR (see Fig. 3).

This diagnostic can in principle measure the radial profile of slow alphas, including also some pitch angle and energy resolution determined by the angle and energy of the diagnostic neutral beam. The principal difficulty is the harsh neutron background expected at $Q \approx 1$. This background can be although its use for alpha diagnostics will require $Q \approx 1$ conditions.

3.3. *Double charge exchange*

The slow confined alphas can also doubly charge exchange with neutral helium atoms introduced either with a diagnostic neutral beam [14] or by recycling in a predominantly helium plasma. Recently Hammett has used the latter technique to measure charge-exchanged ^{3}He tail ions up to an energy of 150 keV in a ^{4}He background plasma in PLT [15]. The fast ^{3}He density was $\approx 10^{12}\,\mathrm{cm}^{-3}$ and the background neutral helium density was $\approx 10^{8}$–$10^{10}\,\mathrm{cm}^{-3}$ in that case.

This diagnostic could in principle measure the radial profile of slow alphas, with pitch angle and energy resolution set by both the diagnostic neutral beam and by the charge exchange analyzer itself. The principal difficulty will again be the neutron background expected at $Q \approx 1$. Various charge exchange analyzers capable of making this measurement already exist on TFTR, although application to alpha measurements will probably require $Q \approx 1$ conditions.

3.4. *Burnup measurements*

The confinement properties of alpha-like 1 MeV tritons and 0.8 MeV ^{3}He created by D/D reactions can be determined through the burnup of these ions in the background deuterium [10, 11]. The fractional burnup can be measured by the ratio of 14 MeV D/T neutrons to 2.5 MeV D/D neutrons (for the triton burnup), or by the ratio of escaping 15 MeV protons to 2.5 MeV neutrons (for the ^{3}He burnup). This result can be compared to the expected $\simeq 1\%$ burnup assuming classical fusion product confinement.

Preliminary measurements of the triton burnup fraction have already been made in TFTR by Nieschmidt [16] and Cecil [17] using foil activation and an NR213 scintillator, respectively, and ^{3}He burnup measurements have already been made in TFTR by Strachan using silicon surface barrier detectors [18]. These measurements will be very useful for providing a global view of fusion product confinement, but will not have the space or time resolution which might be necessary to identify specific anomalous loss mechanisms.

3.5. *Fusion gamma diagnostics*

Gamma rays are emitted during D/T and D/^{3}He fusion reactions, and so can be used to monitor the alpha production rate, especially for the latter reaction which produces no neutrons. Standard sodium iodide and NE226 scintillation detectors have recently been used to look for the 17 MeV gamma during deuterium injection into a ^{3}He plasma [17].

Alpha particles can potentially be diagnosed directly through the gammas emitted during their reactions with tritium or ^{7}Li [19]. The main difficulty with this technique is the large background expected from neutron-induced gammas.

3.6. *ICRF emission*

Superthermal alphas should emit electromagnetic radiation at high harmonics of their gyrofrequency, whereas deuterium ions (which have the same fundamental frequency) should emit predominantly at low harmonics. Detection of this radiation using a standard RF antenna at the plasma boundary has been proposed as an alpha diagnostic [20], and an

charged fusion products with characteristic ICRF emission [21].

The technological requirements for this detection system are relatively simple compared to other potential alpha diagnostic techniques. However, the received radiation will have to be interpreted through theoretical models in order to determine the alpha particle populations. A similar detection system has been used on PDX to examine electromagnetic emission characteristic of fishbone instabilities, and so may also be useful for monitoring alpha particle instabilities at $Q \approx 1$.

4. Physics issues concerning alpha particles in TFTR

The physics issues for alpha particles in TFTR again divide naturally into those "single-particle" effects accessible for study without the use of tritium at $Q \ll 1$, and those effects concerning the "collective" confinement and heating properties of alphas which begin to be accessible at $Q \approx 1$. These physics issues will be reviewed briefly in relation to the available TFTR performance and diagnostics.

4.1. *Tests of the classical single-particle confinement model*

The simple classical alpha confinement model described in Section 2.1 can be used to predict the alpha confinement properties of TFTR; for example, Figure 5 shows the escaping alpha flux vs. pitch angle for two different plasma currents at a position ≈ 20 cm outside the plasma at the bottom of the vessel. Since the escaping alpha detectors described in Section 3.1 should be capable of making absolute flux vs. pitch angle measurements they should be able to check such predictions, at least to within the uncertainty associated with the plasma current and alpha source radial profiles (as estimated from the electron temperature and neutron emission profiles).

Anomalous confinement of alphas could be inferred from the escaping alpha detectors in various ways: for example, the escaping flux might have fast fluctuations (e.g., correlated with MHD activity), the pitch angle distribution might show unexpected flux at large angles (indicating alphas transported to the plasma edge), and/or the expected non-prompt loss at low energies may not appear (indicating spatial loss rates competitive with energy loss rates).

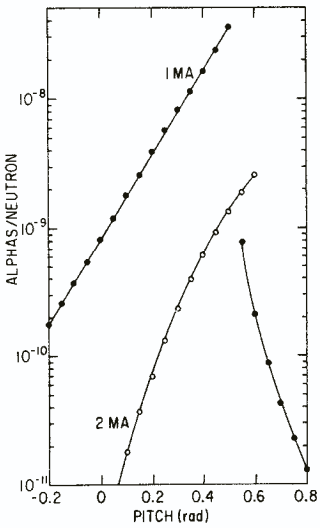

Fig. 5. Predicted escaping alpha flux vs. pitch angle for two plasma currents in TFTR for a detector located 20 cm outside the plasma at the bottom of the vessel. This variation of flux with pitch angle is due to the varying distance of closest approach of the orbits to the plasma center; thus the magnitude of the "jump" at about 0.5 rad (complementary pitch angle) depends on the assumed alpha source profile. [Note that "0" pitch angle in this figure corresponds to an alpha orbit with $v_{tor} = 0$ at the detector.]

Information about the slow confined alphas would also be useful in testing single-particle confinement, since the classical model predicts that nearly all alphas that are confined on their first orbit will remain confined until thermalized. For example, if the local central density of alphas is less than expected, it suggests that these particles anomalously diffuse radially during a slowing down time. Note, however, that the low energy alpha population depends on both the local source rate and also the local slowing down time, so that an unexpected depletion of these particles might also be interpreted as an anomalously fast thermalization. Unfortunately, the charge exchange diagnostics described in Sections 3.2 and 3.3 will probably not be useful at $Q \ll 1$.

More accessible tests of the global confinement of alphas can be made indirectly through the burnup measurements of tritons and ^{3}He as described in Section 3.5. For example, the current dependence of the predicted confined alpha fraction as shown in Fig. 2 should be reflected in the burnup fraction, as already shown on PLT and PDX [10] at relatively low currents. Again this measurement is somewhat ambiguous in that anomalously low burnup can be interpreted either as anomalous loss or anomalously fast thermalization.

Taken together these three techniques should be able to characterize the single-particle alpha confinement at least as well as the neutral beam ion or ICRF tail ion confinement has been characterized to date. The following sections outline some specific physical effects relevant to possible anomalous alpha behavior in TFTR.

4.2. *Ripple effects*

Alphas can be deconfined by toroidal field ripple through three distinct mechanisms: ripple trapping in local magnetic wells [22, 23], diffusion of non-ripple trapped banana orbits by random walks due to ripple at the banana tips [24], and resonance between the alpha gyroorbit and the ripple period [25]. Although these mechanisms were not discussed above, they are also "classical" in the sense that they can be precisely calculated given the magnetic structure of TFTR.

Ripple trapping regions in TFTR exist along the outer half of the plasma typically outside $r/a \approx 0.6$ at 45° from the outer equatorial plane and outside $r/a \approx 1$ at the vessel bottom. All alphas born within these regions with sufficiently large pitch angles will be lost to the wall promptly; however, for normal alpha source profiles this should result in a negligible alpha loss fraction. This ripple loss can be checked using escaping alpha detectors arrayed toroidally across one ripple period.

Ripple-induced diffusion of banana trapped alphas may lead to losses which are spatially modulated with the toroidal ripple period. As calculated recently by White [26], this mechanism ought to rapidly deconfine all alpha in TFTR with banana tips outside a radius typically $r/a \approx 0.6$. These losses might be distinguished from axisymmetric prompt losses as a function of plasma current, since this ripple loss threshold is only weakly dependent on plasma current

The plasma position could also be varied as a test of this mechanism, since the toroidal field ripple is highly in/out asymmetric.

The third ripple loss mechanism requires a resonance between the gyroperiod of an alpha and the transit time across one ripple period. At a toroidal field above ≈ 20 kG this resonant condition can never be satisfied for 3.5 MeV alphas in TFTR; however, this effect can potentially be studied using the faster 3 or 15 MeV protons with the escaping alpha detectors.

4.3. *Sawteeth effects*

The most likely anomalous transport mechanism for alphas would be a spatial redistribution of the confined alphas at sawtooth "crashes", analogous to the redistribution of plasma density and energy. Such a flattening of the fast alpha population is already incorporated into the BALDUR code used to produce Fig. 3.

Such an internal redistribution of confined alphas will not be easy to detect in TFTR. One possible method is to look for modulation in the local density of slow confined alphas with the single or double charge exchange diagnostics (Sections 3.2 and 3.3), noting that the population of slow alphas responds only slowly (over $\approx \tau_{s,e}$) to modulation of the local source function (which is also modulated by the sawteeth). Another possibility is that a radial expulsion of fast confined alphas will move these ions onto escaping alpha orbits; however, to detect these one has to first correct for the modulation of the local source rate due to the sawtooth (which could in principle be done through radially resolved neutron emission measurements).

The basic physical mechanism by which sawteeth interact with alphas deserves further study, since it is not clear that very fast ions will follow small-scale internal magnetic perturbations [27]. The prospects for the approach to ignition will be improved if alphas can be shown to be unaffected by sawteeth.

4.4. *Turbulence effects*

The large gyroradii and banana widths of alphas tend to reduce their interaction with small-scale electrostatic or magnetic turbulence. Mynick and Krommes [28] have shown that the diffusion of fast electrons in a specified turbulent field is reduced relative to the diffusion of low energy electrons by:

$$D_e^{\text{fast}} \approx (1/k_\perp \rho)(1/k_\perp \delta)\, D_e^{\text{slow}} \tag{3}$$

where $k_\perp$ is the typical radial wavenumber of the turbulence and ρ and δ are the gyroradius and banana width of the fast electron. The diffusion of fast alphas should be reduced similarly, which is fortunate since the fast alpha velocity is comparable to electron thermal velocities and the alphas would otherwise diffuse radially at a rate comparable to electrons (i.e., potentially very far during an alpha slowing down time).

Measures of turbulent transport of alphas will be difficult, particularly if this transport involves loss of untrapped fast ions to the inner or outer equatorial plane (since escaping alpha detectors are difficult to operate at these hot spots). Perhaps the best diagnostic would be the burnup fraction of fusion tritons measured at low density, where the cross-section weighted slowing down time might be long compared to a triton confinement time through this mechanism.

4.5. *Collective alpha-induced instabilities*

Several different types of macro- or micro-instabilities can be induced through the collective effects of alphas [22, 29]. Presumably these effects will appear above some threshold values of alpha density, alpha beta, or alpha pressure gradient.

Perhaps the most likely of these instabilities to appear in TFTR is the alpha "fishbone" which, according to a recent estimate by White [26], is destabilized at $\beta_\alpha \approx 2 \times 10^{-3}$ (assuming that the internal kink is also unstable). As shown in Fig. 3, this value for alpha beta is exceeded near the plasma center for typical $Q \approx 1$ TFTR scenarios. This instability might be characterized by ejection of alphas at the outer equatorial plane, modulation of the alpha beta, and by ICRF emission analogously to the neutral beam induced fishbones.

4.6. *Alpha heating*

Alpha heating should be first detectable through measurements of the central electron temperature, since alphas are created with peaked profiles and heat primarily electrons. Simulations of $Q \approx 1$ scenarios such as the medium density case in Table II suggest that the central electron temperature will increase by as much as 30% with the switch from D/D to D/T; however, systematic effects associated with this switch (such as possible changes in confinement with ion mass) might make the interpretation of such measured temperature changes ambiguous.

Perhaps the first hints of alpha heating will come from transient effects such as the delayed decay of the central electron temperature after beam turn-off due to the relatively long slowing down time of alphas compared to neutral beam ions, or from an increased rate of rise of central temperature between sawtooth crashes. The magnitude of such effects will depend in part on the confinement properties of alpha-heated plasmas, which is the principle physics issue to be addressed by the next generation of ignited plasmas.

5. Conclusions

TFTR will be used to study whether alphas and alpha-like fusion products behave according to the predictions of the classical confinement and thermalization models. Several new diagnostics will be developed for these studies, including radiation resistant escaping alpha and slow confined alpha detectors.

Specific physics issues to be addressed include the effects of plasma current, toroidal field ripple, sawteeth, and turbulence on alpha confinement. At its $Q \approx 1$ performance level TFTR can also be used to begin the study of the collective behavior of alpha particles and the effects of alpha heating on plasma confinement.

Acknowledgements

I thank E. Cecil, G. Hammett, W. Heidbrink, D. Mikkelsen, H. Mynick, J. D. Strachan, R. White and K. Young for their contributions to this paper.

References

1. Murphy, T. J. and Strachan, J. D., Nucl. Fus. **25**, 383 (1985).
2. Hively, L. M. and Miley, G. M., Nucl. Fus. **17**, 1021 (1977); also Hively, L. M., Ph.D. thesis, Univ. of Illinois (1980).
3. Mikkelsen, D., Physics of Plasmas in Thermonuclear Regimes, (Edited by B. Coppi and W. Sadowski), DOE Conf. 790866 (1979).
4. Gerdin, G. *et al.*, Fusion Technology **7**, 181 (1985).
5. Post, D. E., Applied Atomic Collision Theory, Academic Press (1984).
6. Mikkelsen, D., Private communication (1986).
7. Post, D. E. *et al.*, J. Fus. Energy **1**, 129 (1981).
8. Zweben, S. J., Redi, M. H. and Bateman, G., Princeton University Report PPPl-2316 (1986).
9. Zweben, S. J., Rev. Sci. Inst. **57**, 1723 (1986).
10. Heidbrink, W. W., Chrien, R. E. and Strachan, J. D., Nucl. Fus. **23**, 917 (1983).
11. Strachan, J. D. *et al.*, Proc. Workshop on Basic Processes in Toroidal Fusion Devices, Varenna (1985) (to be published).
12. Zweben, S. J., Rev. Sci. Inst. **57**, 1774 (1986).
13. Fonck, R. J., Rev. Sci. Inst. **56**, 885 (1985).
14. Post, D. E., Grisham, L. R. and Medley, S. S., Nuclear Tech./Fusion **3**, 457 (1983).
15. Hammett, G., Ph.D. thesis, Princeton Univ. (1986).
16. Nieschmidt, E., Private communication (1986).
17. Cecil, E., Private communication (1986).
18. Strachan, J. D., Rev. Sci. Inst. **57**, 1771 (1986).
19. Cecil, E., Zweben, S. and Medley, S. S., Nucl. Inst. Meth. **A245**, 547 (1986).
20. Moses, K., Private communication (1986).
21. Cottrell, G. A. *et al.*, Proc. 13th Eur. Conf. on Cont. Fus. and Plasma Heating, Schlieresee (1986) (to be published).
22. Kolesnichenko, Y., Nucl. Fus. **20**, 727 (1980).
23. Bittoni, E. and Haegi, M., Eur. Conf. on Plasma Physics, Budapest (1985) (to be published).
24. Goldston, R. J., White, R. B. and Boozer, A. H., Phys. Rev. Lett. **47**, 647 (1981).
25. Putvinskii, S. V. and Shurygin, V. V., Sov. J. Plasma Phys., September–October (1984) 534.
26. White, R. B., private communication (1986).
27. Zweben, S. J. *et al.*, Nucl. Fus. **23**, 477 (1980).
28. Mynick, H. E. and Krommes, J. A., Phys. Fluids **23**, 1229 (1980).
29. Lisak, M., Anderson, D. and Hamnen, H., Phys. Fluids **26**, 3308 (1983).